

CNN based dense underwater 3D scene reconstruction by transfer learning using bubble database

Kazuto Ichimaru[†] Ryo Furukawa[‡] Hiroshi Kawasaki[†]
[†] Kyushu University, Fukuoka, Japan
[‡] Hiroshima City University, Hiroshima, Japan

Abstract

Dense 3D shape acquisition of swimming human or live fish is an important research topic for sports, biological science and so on. For this purpose, active stereo sensor is usually used in the air, however it cannot be applied to the underwater environment because of refraction, strong light attenuation and severe interference of bubbles. Passive stereo is a simple solution for capturing dynamic scenes at underwater environment, however the shape with textureless surfaces or irregular reflections cannot be recovered. Recently, the stereo camera pair with a pattern projector for adding artificial textures on the objects is proposed. However, to use the system for underwater environment, several problems should be compensated, i.e., disturbance by fluctuation and bubbles. Simple solution is to use convolutional neural network for stereo to cancel the effects of bubbles and/or water fluctuation. Since it is not easy to train CNN with small size of database with large variation, we develop a special bubble generation device to efficiently create real bubble database of multiple size and density. In addition, we propose a transfer learning technique for multi-scale CNN to effectively remove bubbles and projected-patterns on the object. Further, we develop a real system and actually captured live swimming human, which has not been done before. Experiments are conducted to show the effectiveness of our method compared with the state of the art techniques.

1. Introduction

Dense 3D shape acquisition of swimming human or live fish is an important research topic for sports, biological science and so on. Passive stereo is a common solution for capturing 3D shapes because of its advantage on simplicity; i.e., it only requires two cameras. In addition, since the shapes are recovered only from a pair of stereo images, it can capture moving or deforming objects. One severe problem on passive stereo is instability, i.e., it fails to cap-

ture objects with textureless surfaces or irregular reflection. To overcome the problem, using a pattern projector to add an artificial texture onto the objects has been proposed. At underwater environments, there are additional problems for shape reconstruction by the system, such as refraction and disturbance by fluctuation and bubbles. Further, since original textures of objects are interfered by bubbles and projected patterns, they should be removed for obtaining original texture. For refraction issue, a depth-dependent calibration where refractions are approximated by a lens distortion of a center projection model is proposed [16]. For disturbance issue, recently a convolutional neural network (CNN)-based stereo is proposed [11]. However, those previous techniques still have some holes in their results when bubble size is large, because the shapes are irregular and partially transparent. In addition, all the experiments are only conducted with a small water tank under controlled lighting condition.

In this paper, we propose a transfer learning based CNN stereo as well as efficient construction of bubble database for the purpose; we develop a special bubble generation device to create a bubble database containing multiple size and density of bubbles. For the texture recovery, we also propose a CNN-based method for projected-pattern removal and bubble-canceling method. Since it is great labor to prepare task-specific dataset in extreme environment, we develop an unsupervised learning approach for texture recovery. Further, we develop a real system to capture live swimming human in a pool where lighting and other conditions are unknown and cannot be controlled.

Experimental results are shown to prove the effectiveness of our method by comparing the results with the previous methods [6, 11, 36]. We also conduct demonstration to show the reconstructed sequence of swimming human. Main contributions of the proposed technique are as follows:

1. A multi-scale CNN-based stereo with transfer learning technique specialized for underwater environment is proposed.

2. An unsupervised multi-scale CNN-based bubble and projected pattern removal method specialized for underwater environment is proposed
3. A special bubble generation device to create original database containing wide variety of bubble for transfer learning are developed; the database is plan to be public available.
4. The proposed technique is applied to live swimming human to recover the dynamic 3D shapes to confirm feasibility and practicability of the method.

2. Related work

For refraction problem, there are generally two types of solutions; one is geometric approach and the other is approximation-based approach. Geometric approach is based on physical models such as refractive index, distance to refraction interface, and normal of the interface [2, 14, 15]. Those techniques can calculate genuine light rays if parameters are correctly estimated and interface is completely planar, however, they are usually impractical. Further, the non-central projection camera model is not suitable for shape reconstruction in theory. On the other hand, approximation approach converts captured images into central projection images by lens distortion and focal length adjustment [8]. They assumed focal point moved backward to adjust light paths to be as linear as possible, then remaining error was treated as lens distortion. It works well in most cases, but in specific case it fails because refractive distortion depends on depth and effective range of depth is not thoroughly analyzed yet.

In terms of light attenuation and disturbance problem for water medium, light transport analysis has been conducted [28, 25]. Narasimhan *et al.* proposed a structured-light-based 3D scanning method for strong scattering and absorption media based on light transport analysis [27]. For weak scattering media, Bleier and Nüchter used cross laser projector which only achieved sparse reconstruction [4]. To increase density, Campos and Codina projected parallel lines with DOE to capture underwater objects with one-shot scan [23]. Kawasaki *et al.* proposed a grid pattern to capture more dense shape with one-shot scan [16]. One drawback of those one-shot scanning techniques is that reconstruction tends to be unstable even if light attenuation and disturbances are not so strong because sensitivity of pattern detection is high for subtle change of projected pattern. Some research such as [3] used infrared structured light or ToF sensors, but infrared attenuates rapidly in water as shown in Fig. 1, and is not practical.

One simple solution is to apply passive stereo which is not much affected by those effects. In the air, to increase the stability, Konolige investigated how to add active pattern to the passive stereo system [18] and there are also commercial products available [1, 13]. We focus its simplicity and

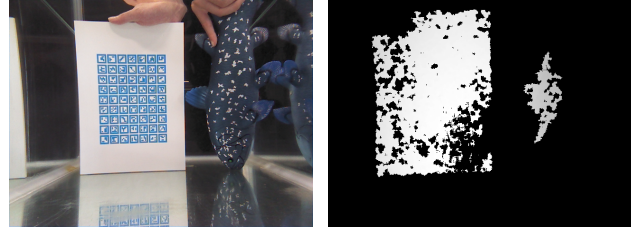


Figure 1. Captured RGB image and depth image by Kinect v1. Distance to the targets is 70cm.

stability to achieve dense dynamic reconstruction.

Recently, convolutional neural network (CNN) based stereo matching becomes popular. Žbontar and LeCun proposed a CNN-based method to train network as a cost function of image patches [36]. Those techniques rather concentrate on textureless region recovery, but not noise compensation, which is a main problem for underwater stereo. Since patch based technique is known to be slow, Luo *et al.* proposed a speeding-up technique by substituting FCN to inner product at final stage [22]. Shaked and Wolf achieve high accuracy as well as fast calculation time by combining both FCN to inner product [30]. To fundamentally solve the calculation time, end-to-end approach called DispNet is proposed, but accuracy is not so high [24]. Another problem for patch based CNN stereo is that it is severely affected by obstacles, image degradation or various scaling. Recently, multi-scale CNN technique is proposed to solve the patch size problem. Nah *et al.* proposed a method for dehaze [5] and Li *et al.* proposed a method for object recognition [19], and Yadati *et al.*, Lu *et al.*, Chen *et al.*, and Ye *et al.* [33, 21, 7, 34] used multi-scale features for CNN-based stereo matching. Chang and Chen extended multi-scale CNN stereo to end-to-end network called PSMNet [6], and achieved higher accuracy, but handleable resolution is very limited because of huge memory consumption. Ichimaru *et al.* used FCN after multi-scale feature extraction to wisely integrate them [11], but they used only general stereo dataset.

Collection of huge data for learning is another open problem for CNN-based stereo techniques. For solution, Zhou *et al.* proposed a technique without using ground truth depth data, but LR consistency as a loss function [37]. Tonioni *et al.* proposed a unsupervised method by using existing stereo technique as an instruction [31]. Tulyakov and Ivanov proposed a multi-instance learning (MIL) method by using several constraints and cost functions [32]. However in general, unsupervised learning is instable compared to supervised learning. DispNet [24] and PSMNet [6] are trained with generated images based on computer graphics, but transfer learning with natural images is necessary since computer graphics is not realistic enough to learn noises or

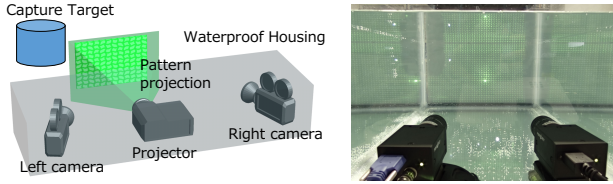


Figure 2. **Left:** Minimum system configuration of the proposed algorithm. **Right:** Our experimental system for evaluation where two cameras and a projector are set outside a water tank.

camera characteristics. In this research, we created original stereo dataset and a special device for data augmentation which reproduces underwater environment for transfer learning.

CNNs are also popular in the field of image restoration and segmentation. In underwater environment, there are several noises, such as bubbles or shadows of water surfaces. In addition, projected pattern onto the target object is also a severe noise. To remove such a large noise, inpainting method based GAN is promising [12, 35]. However, since resolution of generative approach is basically low, noise removal approach is better fit to our purpose. For efficient noise removal, shallow CNN based approach using residual is proposed [9]. Liu and Fang propose end-to-end architecture using WIN5RB network [20] which outperform others. We also use this technique, but data collection and multi-scale extension is our original. Further, we also propose unsupervised learning approach to overcome the difficulties preparing such task-specific dataset.

3. System and algorithm overview

3.1. System Configuration

The proposed system includes two cameras and one projector as shown in Fig. 2. We prepare two systems for experiments. One is for evaluation purpose where two cameras and a projector are set outside a water tank. The other is a practical system where devices are installed into a waterproof housing. For the both systems, the optical axes of the cameras are set orthogonal to housing surface so that error by refraction approximation is minimized. The two cameras are synchronized to capture dynamic scenes. In terms of the pattern projector to add textures onto the objects, no synchronization is required since the pattern is static.

3.2. Algorithm

The flow of our algorithm is shown in Fig. 3. In learning phase, several CNNs such as CNN-based segmentation, CNN-based stereo matching, and CNN-based texture recovery are trained for robustness against underwater disturbances as shown in Fig. 3 (top). First, CNN-based segmentation network is trained to detect reconstruction target region. It can be trained with large image dataset, or

small dataset created from captured images in reconstruction phase. In the method, we manually created the mask data for learning. For CNN Stereo, proper stereo dataset suitable for assuming application is prepared (*e.g.*, fish and human images, in our case) without bubble. We also create special dataset which reproduces underwater environment by using a special bubble generation device for transfer learning purpose. CNN-based stereo matching network is efficiently trained by using both datasets. CNN-based texture recovery networks are also trained with prepared dataset.

Reconstruction process is shown in Fig. 3 (bottom). First, the camera pair is calibrated. The refractions in the captured images are modeled and canceled by center projection approximation by depth-dependent calibration [16]. In the measurement process, the targets are captured with stereo cameras. Pattern illumination is projected onto the scene for adding features on it. From captured images, target regions are detected by a CNN-based segmentation technique, where only target regions are extracted. Then, a stereo-matching method is applied to the target regions. In our technique, a CNN-based stereo is applied to increase stability under the condition of dimmed patterns, disturbances by bubbles, and flickering shadows. Then, 3D points are reconstructed from disparity maps estimated by the stereo algorithm. Outliers are removed from the point cloud and meshes are recovered by Poisson equation method [17]. Since textures are degraded by bubbles and projected patterns, they are efficiently recovered by CNN-based bubble canceling and pattern removal technique. Using the recovered 3D shapes and textures, we can render the dynamic and textured 3D scene.

4. Stereo reconstruction using CNNs

To deal with bubbles and water fluctuation disturbing the images, we create special database containing multiple size and density of bubbles at real underwater environment for transfer learning (Sec. 4.1). By using the data, we apply CNN-based target region extraction technique (Sec. 4.2) and multi-scale CNN stereo (Sec. 4.3).

4.1. Underwater stereo dataset created by special bubble generation device

First, we create basic training datasets for stereo with projected pattern as follows. Since we assume measurement of swimming human and fish as our purpose, dataset which includes fish-like and human skin-like objects is necessary. Thus, we prepared model of coelacanth, largemouth bass, goliath grouper, mannequin head and hand. We prepared two cameras and one projector, and captured the above models and some additional objects in the air with gray-code techniques from two views. Then we captured targets with two cameras changing room illumination and pattern

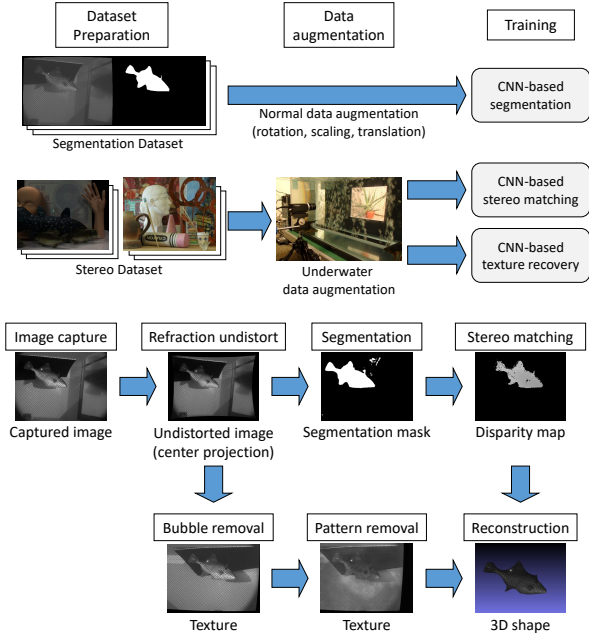


Figure 3. Overview of the algorithm.

projection condition. We captured 8 target object set, 3 poses, 3 illumination, and 4 pattern projection condition, in total 288 stereo image pairs were acquired. We also created ground truth disparity map from captured graycode images as shown in Fig. 6 (right). The dataset is named “Coel Dataset”. An example of the image in the dataset is shown in Fig. 6 (left).

Then, we create special training datasets for underwater stereo as follows. To effectively train the network with scene include bubbles, we develop a special bubble generator to reproduce underwater environment (Fig. 4). Since underwater bubbles have wide variety, it is necessary to generate various types of bubbles. Our bubble generator can control bubble size, density, and generating position. We used the device to augment stereo dataset with bubble. Then, we placed a camera and a LCD monitor as they face each other, and placed water tank of $90 \times 45 \times 45$ cm in-between them. Water tank was filled with transparent water and bubble generator is submerged into the tank. Graycode patterns were presented on the monitor and captured by the camera in order to acquire 2D point correspondences between camera image plane and the monitor pixel position. Then, arbitrary images of public available dataset were displayed on the monitor and captured by the camera while bubbles are generated in the tank. We captured dataset in 2 bubble sizes, 2 generating positions and 2 densities, *i.e.*, total 8 cases plus one no-bubble scene as shown in Fig. 5. Used images are Middlebury 2005, 2006 dataset and Coel Dataset which contains 918 images. Note that such underwater stereo datasets including real bubbles do not yet exist

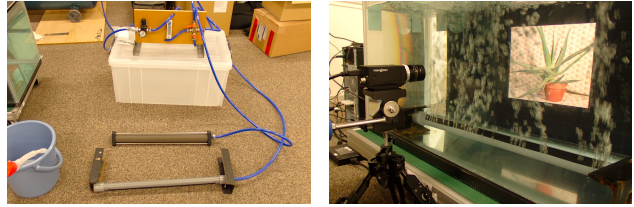


Figure 4. **Left:** Appearance of bubble generator. **Right:** Situation of bubble data augmentation.

and we will make the datasets public available; this is one of our important contribution of the paper.

4.2. CNN-based target-region extraction

For many applications, reconstruction targets are recognizable, such as swimming human in the water. In general, the wider the range of disparities considered in stereo-matching processes, the more possibilities exist, leading to wrong correspondences. Thus, by extracting the target regions from the input images and reducing possibilities of matching outside the target regions, 3D reconstruction process becomes more robust. In addition, 3D points of only required region can be obtained.

To this purpose, we implemented an U-Net [29], an FCN with multi-scale feature extraction, and trained it for this task. We made training dataset from underwater image sequences. From image sequences, 200 images were sampled and the target regions were masked with manual operations. These training images were augmented by scalings, rotations, and translations. As a result, we provide 2000 pairs of source images and target-region masks for training U-Net. We use cross entropy as loss function. The trained U-Net is tested for large number of images, we obtained qualitatively successful results in most examples, even when camera was moving during capturing (Fig. 7).

In the evaluation process, we have found that the numbers of resolution levels of the U-Net architecture is important. By using only two or three levels of resolutions, we could not get sufficient results. We finally reached the conclusion that the U-Net with five levels of resolutions works effectively with our dataset.

Using the obtained results, disparity search range can be limited and which improves robustness. The search range limitation is implemented into CNN stereo matching described later, which takes mask images as input in addition to rectified images.

4.3. Multi-scale CNN stereo for robustness against bubble

There are several peculiar phenomena in the water such as bubbles, shadows of water surface, refraction caused by difference of water temperature, and so on. Those phenomena degrade the captured image and make bad effects on

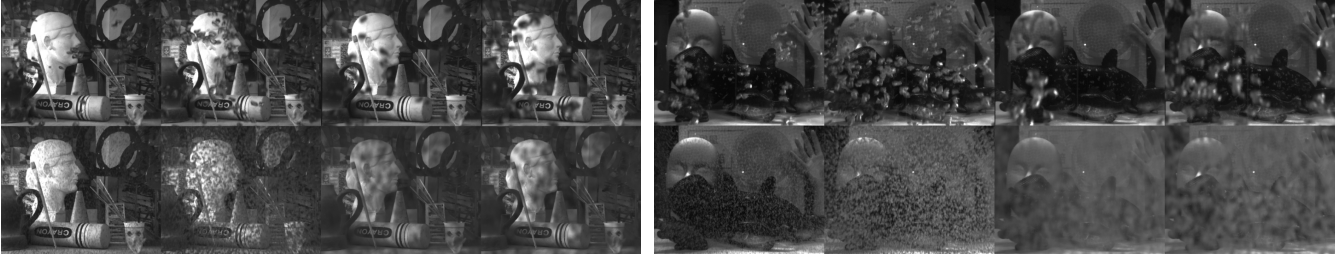


Figure 5. Examples of augmented dataset with various types of bubbles.

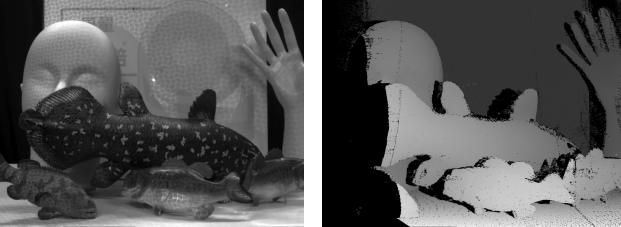


Figure 6. **Left:** An example of images included in Coel Dataset. **Right:** An example of disparity map.



Figure 7. An example of CNN segmentation results.

stereo matching. Since those phenomena are explained by complicated process of both physics and optics, it is difficult to solve analytically. In the paper, we adopt a learning based approach, *i.e.*, CNN, for solution.

Since bubbles and water fluctuation have much larger structure than pixel scale, basic CNN-based stereo matching technique does not work [36]. There are several papers which can handle a large spatial structure by multi-scale extension [33, 21, 7] and they can recognize large scale information, however, such previous methods does not use enough number of scales, or utilize multi-scale information due to flattening of multi-scale features. In the paper, we propose multi-scale CNN stereo architecture which takes multiple scale patches (more than three) and process the retrieved features by Fully Convolutional Networks (FCN); this is not common for multi-scale CNN stereo. The architecture is shown in Fig. 8. It takes 44×44 (the size depends on the number of scales) patches from left and right rectified images for calculation. In the matching process, first, patches are down-sampled by MaxPooling layers, and multiple scale patches are prepared. Second, each patch is processed by former FCN to retrieve multi-scale features, respectively. Then, retrieved multi-scale features are up-sampled to original scale, concatenated, and processed by FCN to integrate multi-scale information. Finally, output tensors are vectorized and cosine distance between left and right vector is calculated to determine the similarity score.

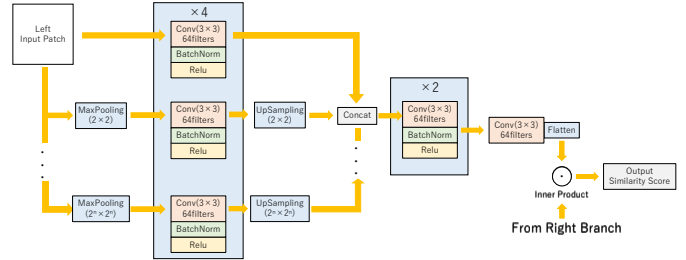


Figure 8. Network architecture of multi-scale CNN stereo. Left and right branches are symmetry.

Weights are shared between left and right branches to reduce memory consumption, because multi-scale CNN architecture tend to consume large memory. Cost volume is obtained by sweeping input images with patches.

Finally, post-processing are applied such as Semi-Global Matching (SGM) [10] as well as Left-Right consistency check to get final disparity map. Post-processing is implemented by GPU and it achieved fast calculation as mentioned in experiment section. Effectiveness of our architecture is confirmed in experiment section (Sec. 6.1).

5. Unsupervised texture recovery from bubble and projected pattern

For real situations, the captured images are often severely degraded by underwater environments, such as bubble and other noises, as well as projected pattern on the object surface. In order to remove such undesirable effects, we propose CNN-based solution. In our technique, we focus on two major problems, such as bubbles and projected pattern. Although those two phenomena are totally different and have different optical attributes, it is common in the sense that appearances for both effects have a wide variation in scale. Note that such wide variation depends on the distance between a target object, bubble and a projector. Such a large variation of scale of them makes it difficult for removal by simple noise removal method.

Since multi-scale CNN is suitable to learn such a variation, we also use a multi-scale CNN for our bubble and pattern removal purpose. The network for such obstacle removal is shown in Fig. 9. In the figure, it is shown that an

original image is converted to three different resolutions and trained by independent CNN. Each output is up-sampled and concatenated to higher resolution. This network is advantageous because it can handle a large structure of projected pattern, as well as it can be trained in a relatively short time.

For pattern removal training phase, we also used Coel Dataset as pattern removal training data which contains both images with and without pattern on same scene. We used images with pattern as input, and images without pattern as ground truth. Ground truth images were adjusted their brightness and contrast to fit to input images. In addition, although we need to remove projected pattern on real fish, Coel Dataset does not contain such images. Thus, we prepared raw fish (sea bream, filefish and chicken grunt) and submerged them into the water, then we captured them with and without pattern to make transfer dataset. The pattern removal network was trained with the transfer dataset after trained with Coel Dataset. In terms of bubble removal training, we used bubble augmented stereo dataset aforementioned in Sec. 4.1 using no-bubble scene as ground truth.

Furthermore, we consider unsupervised learning approach to recovery correct texture even in case training dataset is insufficient. To achieve it on pattern removal, first we trained pattern detection network to output the difference image between with and without pattern. The network architecture is duplication of texture recovery network shown in Fig. 9. It can be trained in insufficient dataset situation because pattern detection is easier than pattern removal, or we can use alternative pattern detection method if necessary as [16]. Using pattern detection network, loss function is defined as below:

$$MSE(in, R(in)) + \lambda \times MSE(D(R(in)), \vec{0})$$

where in means input image, R and D means output of pattern removal and detection respectively, MSE means mean squared error, and λ is coefficient for balancing. The loss function leads to pattern is not detected, *i.e.*, pattern is removed, while keeping output image not far from input image. Result of the function is back-propagated to only pattern removal network. The network was also trained with Coel Dataset and fish transfer dataset. Effectiveness of this unsupervised learning is confirmed in experiment section (Sec. 6.2).

6. Experiments

In order to evaluate our proposed method, we conducted several experiments. First, robustness of Multi-scale CNN stereo against underwater disturbances is investigated in Sec. 6.1. Then, qualitative evaluation of texture recovery is conducted in Sec. 6.2. Finally, we captured real swimming human sequence and reconstructed it by proposed method to confirm its feasibility in Sec. 6.3.

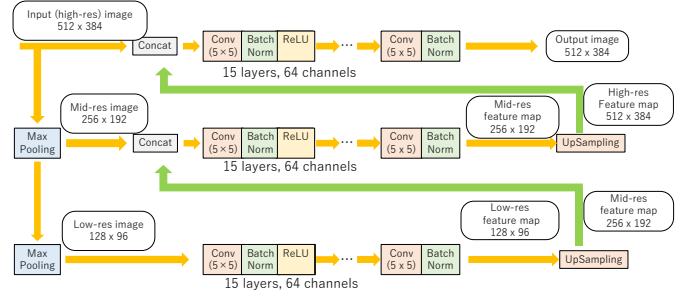


Figure 9. Network architecture of multi-scale CNN texture recovery.

6.1. Evaluation of various CNN stereo techniques

We tested CNN-based stereo for underwater scene with bubbles. For evaluation purpose, we prepared six implementations, such as single-scale CNN stereo of [36] (mc-cnn), 2-scale CNN stereo with linear combination of [7] (ms-cnn-lin), end-to-end multi-scale CNN stereo of [6] (PSMNet), 2-scale CNN stereo with FCN of [11] (ms-cnn-fcn-2), proposed 3-scale CNN stereo with FCN (ms-cnn-fcn-3), and transfer learned ms-cnn-fcn-3 with bubble images (ms-cnn-fcn-3 (trans)). All CNNs were implemented with Tensorflow and trained with Middlebury 2001, 2003, 2005, 2006, 2014, and Coel Dataset, except ms-cnn-fcn-3 (trans) was also trained with augmented dataset, and pre-trained model (KITTI 2015) was used for PSMNet. Post-processing such as SGM and LR Check were implemented with CUDA and achieved processing 1024×768 px images (maximum disparity is 256) in 30 seconds.

The target objects were placed at a distance of 50, 60, 70cm and the depth-dependent calibration was applied. We intentionally made bubbles to interfere image capturing process. We reproduced four bubble environments, *i.e.*, far little bubble, far much bubble, near little bubble, and near much bubble. In addition, no bubble scenes as reference were prepared. We captured three pairs of images for each target with five environments. In total, 90 images were captured. Then, we calculated disparity map by each CNN methods, and reconstructed all the scenes and targets. We calculated average RMSE from the GT shape of each target.

The results are shown in Fig. 13. From the graph, we can confirm that the accuracy of proposed CNN architecture is better than previous method, supporting the effectiveness of our method. Fig. 11 shows examples of the reconstructed disparity maps for each technique confirming that shapes are recovered by our technique even if captured images are severely degraded by bubbles. Further comparison between PSMNet [6] and ours are shown in Fig. 10. PSMNet had difficulty to estimate correct disparity especially when the region was in occluding boundary, whereas ours estimated correct results.

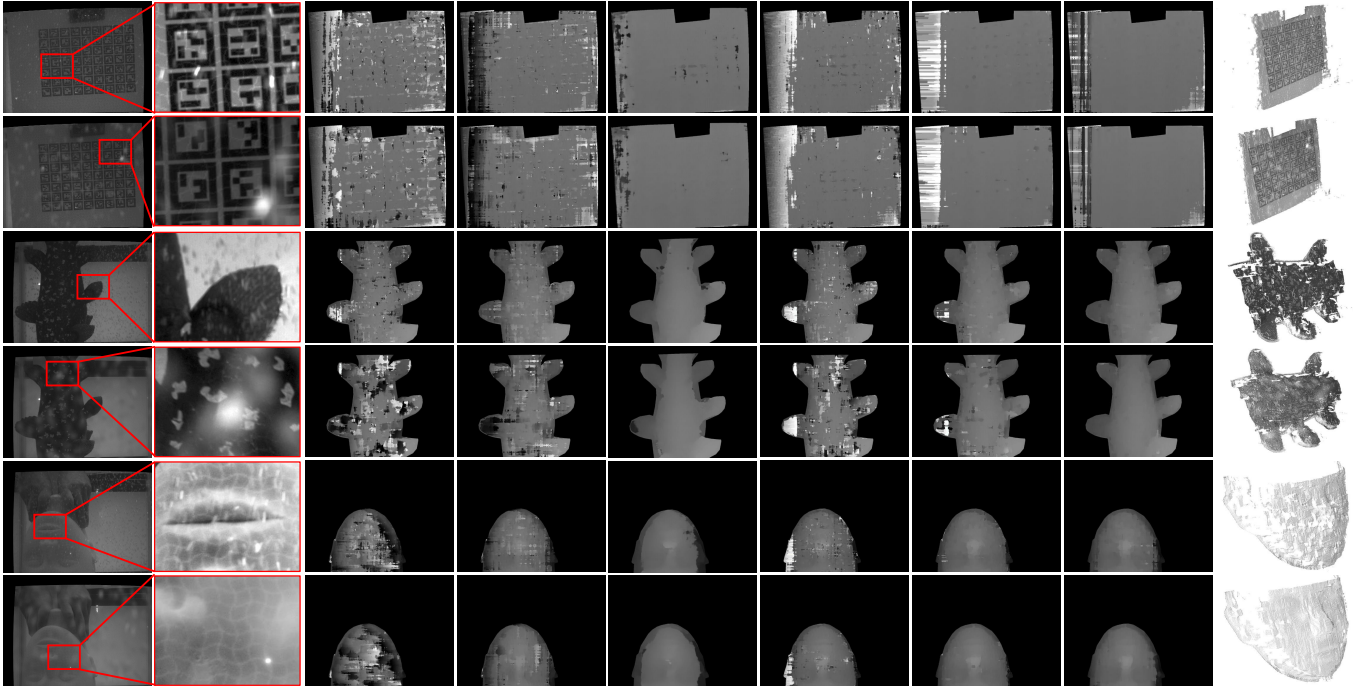


Figure 10. Difference of disparity map between stereo methods in bubble scene. **Left to Right:** Input image with bubbles, close-up of input, mc-cnn results [36], ms-cnn-lin results [7], PSMNet results [6], ms-cnn-fcn-2 results [11], ms-cnn-fcn-3 results, ms-cnn-fcn-3 (trans) results and reconstructed point cloud.

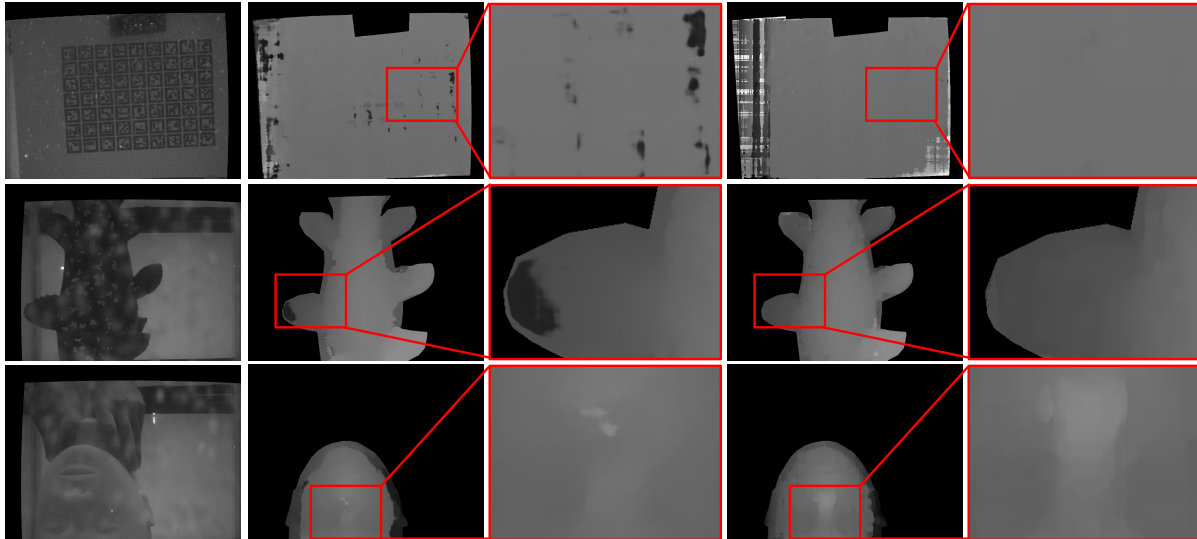


Figure 11. Detailed comparison of disparity map between PSMNet and ours. **Left to Right:** Input image, PSMNet results, close-up of PSMNet results, ms-cnn-fcn-3 (trans) results, and close-up of ours.

6.2. Experiments of texture recovery

We also tested the bubble-removal and the pattern-removal techniques. The results are shown in Fig. 14. We can confirm that projected patterns are robustly removed by multi-scale CNN technique. Top two rows are results of supervised learning, and bottom row is result of unsupervised learning, showing unsupervised learning has enough ability to remove pattern.

6.3. Demonstration with swimming human

Finally, we captured swimming human in a swimming machine, where swimmer can keep the same position by artificially created water flow. We made special experimental system, which consists of low-cost commercial devices, such as GoPro Hero 3+ for stereo camera pair with synchronous cable, and a laser pattern projector with battery (Fig. 15). We captured several swimming sequences, which

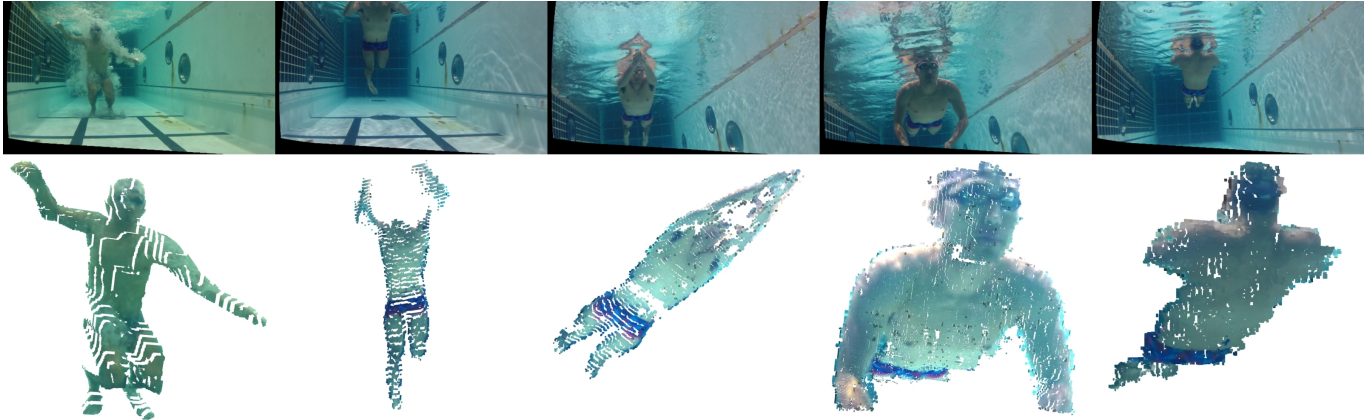


Figure 12. Swimming human experiment. Images are too small and only the left-most image shows significant bubbles, but all images contain bubbles in captured images.

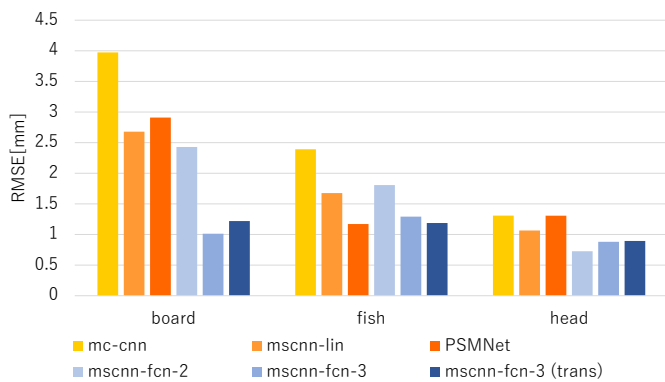


Figure 13. Comparison on proposed methods (blue bar) and previous methods (red bar). Proposed methods performed best in most cases.

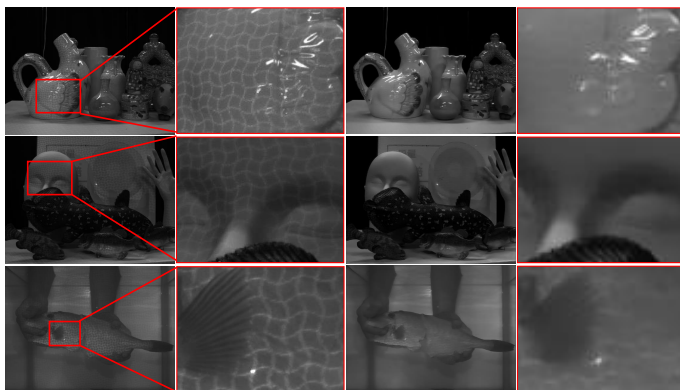


Figure 14. Result of texture recovery experiment. first column is input image, 2nd column is close-up of input, 3rd column is output image, 4th column is close-up of output.

is 3920 frames in 24 frames per seconds, *i.e.*, 163 seconds in total. The reconstructed results are shown in Fig. 12. In the figure, we can confirm that the 3D shape of human is successfully reconstructed by our method, even when the body was covered in heavy bubbles. Since direction of optical axis of camera is almost parallel to human axis in this

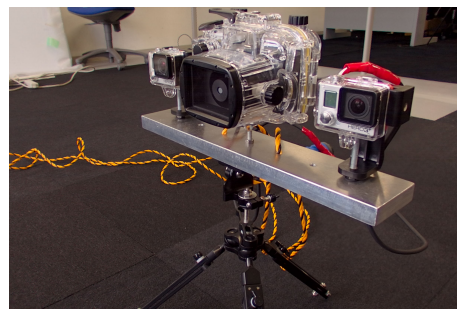


Figure 15. Experimental rig for swimming human capture.

setup, reconstructed depth is largely discretized; solution is our important future work.

7. Conclusion

In this paper, we propose a robust and practical underwater dense shape reconstruction method using stereo cameras with a static-pattern projector. Since underwater environments have severe conditions, such as refraction, light attenuation and disturbances by bubbles, we propose a CNN-based solution, such as target-object segmentation and robust stereo matching with a multi-scale CNN. To acquire task-specific dataset, we created stereo dataset and special device for data augmentation which reproduces underwater environment. We also propose a texture-recovery method using a CNN. With our method, images with strong bubbles are robustly recovered through comprehensive experiments showing effectiveness of our method. Our future plan is to create underwater unmanned autonomous vehicle equipped with our system.

Acknowledgment

This work was part supported by grant JSPS/KAKENHI 16H02849, 16KK0151, 18H04119, 18K19824 in Japan, and MSRA CORE14.

References

- [1] 3dMD. 3dMDface System.
- [2] A. Agrawal, S. Ramalingam, Y. Taguchi, and V. Chari. A theory of multi-layer flat refractive geometry. In *CVPR*, 2012.
- [3] A. Anwer, S. S. A. Ali, A. Khan, and F. Mériaudeau. Underwater 3-d scene reconstruction using kinect v2 based on physical models for refraction and time of flight correction. *IEEE Access*, 5:15960–15970, 2017.
- [4] M. Bleier and A. Nüchter. Low-cost 3d laser scanning in air or water using self-calibrating structured light. *International Archives of the Photogrammetry, Remote Sensing and Spatial Information Sciences*, XLII-2/W3:105–112, February 2017.
- [5] Z. Cai, Q. Fan, R. S. Feris, and N. Vasconcelos. A unified multi-scale deep convolutional neural network for fast object detection. In *ECCV*, 2016.
- [6] J.-R. Chang and Y.-S. Chen. Pyramid stereo matching network. In *Proceedings of the IEEE Conference on Computer Vision and Pattern Recognition*, pages 5410–5418, 2018.
- [7] J. Chen and C. Yuan. Convolutional neural network using multi scale information for stereo matching cost computation. In *Image Processing (ICIP)*. IEEE, 2016.
- [8] R. Ferreira, J. P. Costeira, and J. A. Santos. Stereo reconstruction of a submerged scene. In *Pattern Recognition and Image Analysis*, pages 102–109. Springer, 2005.
- [9] K. He, X. Zhang, S. Ren, and J. Sun. Deep residual learning for image recognition. In *IEEE Conference on Computer Vision and Pattern Recognition (CVPR)*, 12 2016.
- [10] H. Hirschmüller. Stereo processing by semiglobal matching and mutual information. *IEEE Transactions on Pattern Analysis and Machine Intelligence*, 30(2):328–341, February 2008.
- [11] K. Ichimaru, R. Furukawa, and H. Kawasaki. Multi-scale cnn stereo and pattern removal technique for underwater active stereo system. In *International Conference on 3D Vision*, 2018.
- [12] S. Iizuka, E. Simo-Serra, and H. Ishikawa. Globally and locally consistent image completion. *ACM Trans. Graph.*, 36(4):107:1–107:14, July 2017.
- [13] Intel. Intel RealSense SR300, 2015.
- [14] A. Jordt-Sedlazeck and R. Koch. Refractive structure-from-motion on underwater images. In *Computer Vision (ICCV), 2013 IEEE International Conference on*, pages 57–64. IEEE, 2013.
- [15] R. Kawahara, S. Nobuhara, and T. Matsuyama. A pixel-wise varifocal camera model for efficient forward projection and linear extrinsic calibration of underwater cameras with flat housings. In *Computer Vision Workshops (ICCVW), 2013 IEEE International Conference on*, pages 819–824. IEEE, 2013.
- [16] H. Kawasaki, H. Nakai, H. Baba, R. Sagawa, and R. Furukawa. Calibration technique for underwater active oneshot scanning system with static pattern projector and multiple cameras. In *Winter Conference on Applications of Computer Vision*, 2017.
- [17] M. Kazhdan, M. Bolitho, and H. Hoppe. Poisson surface reconstruction. In *Proceedings of the fourth Eurographics symposium on Geometry processing*, SGP '06, pages 61–70, 2006.
- [18] K. Konolige. Projected texture stereo. In *International Conference on Robotics and Automation*, pages 148–155. IEEE, 2010.
- [19] B. Li, W. Ren, D. Fu, D. Tao, D. Feng, W. Zeng, and Z. Wang. Reside: A benchmark for single image dehazing. *arXiv preprint arXiv:1712.04143*, 2017.
- [20] P. Liu and R. Fang. Wide inference network for image denoising. *CoRR*, abs/1707.05414, 2017.
- [21] H. Lu, H. Xu, L. Zhang, and Y. Zhao. Cascaded multi-scale and multi-dimension convolutional neural network for stereo matching, 2018.
- [22] W. Luo, A. G. Schwing, and R. Urtasun. Efficient deep learning for stereo matching. In *2016 IEEE Conference on Computer Vision and Pattern Recognition (CVPR)*, pages 5695–5703, June 2016.
- [23] M. Massot-Campos and G. Oliver-Codina. Underwater laser-based structured light system for one-shot 3d reconstruction. In *SENSORS, 2014 IEEE*, pages 1138–1141. IEEE, 2014.
- [24] N. Mayer, E. Ilg, P. Häusser, P. Fischer, D. Cremers, A. Dosovitskiy, and T. Brox. A large dataset to train convolutional networks for disparity, optical flow, and scene flow estimation. In *2016 IEEE Conference on Computer Vision and Pattern Recognition, CVPR 2016, Las Vegas, NV, USA, June 27-30, 2016*, pages 4040–4048. IEEE Computer Society, 2016.
- [25] Y. Mukaigawa, Y. Yagi, and R. Raskar. Analysis of light transport in scattering media. In *Computer Vision and Pattern Recognition (CVPR), 2010 IEEE Conference on*, pages 153–160. IEEE, 2010.
- [26] S. Nah, T. H. Kim, and K. M. Lee. Deep multi-scale convolutional neural network for dynamic scene deblurring. In *The IEEE Conference on Computer Vision and Pattern Recognition (CVPR)*, July 2017.
- [27] S. G. Narasimhan, S. K. Nayar, B. Sun, and S. J. Koppal. Structured light in scattering media. In *Computer Vision, 2005. ICCV 2005. Tenth IEEE International Conference on*, volume 1, pages 420–427. IEEE, 2005.
- [28] M. O’Toole, J. Mather, and K. N. Kutulakos. 3d shape and indirect appearance by structured light transport. *IEEE Transactions on Pattern Analysis and Machine Intelligence*, 38:1298–1312, 2016.
- [29] O. Ronneberger, P. Fischer, and T. Brox. U-net: Convolutional networks for biomedical image segmentation. In *International Conference on Medical Image Computing and Computer Assisted Intervention*, pages 234–241. Springer, 2015.
- [30] A. Shaked and L. Wolf. Improved stereo matching with constant highway networks and reflective confidence learning. In *2017 IEEE Conference on Computer Vision and Pattern Recognition, CVPR 2017, Honolulu, HI, USA, July 21-26, 2017*, pages 6901–6910. IEEE Computer Society, 2017.
- [31] A. Tonioni, M. Poggi, S. Mattoccia, and L. D. Stefano. Unsupervised adaptation for deep stereo. In *2017 IEEE International Conference on Computer Vision (ICCV)*, volume 00, pages 1614–1622, Oct. 2018.

- [32] S. Tulyakov, A. Ivanov, and F. Fleuret. Weakly supervised learning of deep metrics for stereo reconstruction. In *2017 IEEE International Conference on Computer Vision (ICCV)*, pages 1348–1357, Oct 2017.
- [33] P. Yadati and A. M. Namboodiri. Multiscale two-view stereo using convolutional neural networks for unrectified images. In *15th IAPR International Conference on Machine Vision Applications (MVA)*, pages 320–323. IEEE, 2017.
- [34] X. Ye, J. Li, H. Wang, and H. H. adn Xiaolin Zhang. Efficient stereo matching leveraging deep local and context information. *IEEE Access*, 5:18745–18755, 2017.
- [35] C. You, Q. Yang, H. Shan, L. Gjestebj, G. Li, S. Ju, Z. Zhang, Z. Zhao, Y. Zhang, W. Cong, and G. Wang. Structure-sensitive multi-scale deep neural network for low-dose ct denoising, 2018.
- [36] J. Žbontar and Y. LeCun. Stereo matching by training a convolutional neural network to compare image patches. *Journal of Machine Learning Research*, 17:2287–2318, January 2016.
- [37] C. Zhou, H. Zhang, X. Shen, and J. Jia. Unsupervised learning of stereo matching. In *2017 IEEE International Conference on Computer Vision (ICCV)*, pages 1576–1584, Oct 2017.